
EARLY PREDICTION OF RESPIRATORY FAILURE IN THE INTENSIVE CARE UNIT

Matthias Hüser *
Department of Computer Science
ETH Zürich
Zürich, Switzerland

Martin Faltys *
Department of Intensive Care Medicine
University Hospital
University of Bern
Bern, Switzerland

Xinrui Lyu *
Department of Computer Science
ETH Zürich
Zürich, Switzerland

Chris Barber
Department of Computer Science
ETH Zürich
Zürich, Switzerland

Stephanie L. Hyland
Microsoft Research
Cambridge, United Kingdom

Tobias M. Merz †
Cardiovascular Intensive Care Unit
Auckland City Hospital
Auckland, New Zealand

Gunnar Rätsch †
Department of Computer Science
ETH Zürich
Zürich, Switzerland

ABSTRACT

The development of respiratory failure is common among patients in intensive care units (ICU). Large data quantities from ICU patient monitoring systems make timely and comprehensive analysis by clinicians difficult but are ideal for automatic processing by machine learning algorithms. Early prediction of respiratory system failure could alert clinicians to patients at risk of respiratory failure and allow for early patient reassessment and treatment adjustment. We propose an early warning system that predicts moderate/severe respiratory failure up to 8 hours in advance. Our system was trained on HiRID-IL, a data-set containing more than 60,000 admissions to a tertiary care ICU. An alarm is typically triggered several hours before the beginning of respiratory failure. Our system outperforms a clinical baseline mimicking traditional clinical decision-making based on pulse-oximetric oxygen saturation and the fraction of inspired oxygen. To provide model introspection and diagnostics, we developed an easy-to-use web browser-based system to explore model input data and predictions visually.

1 Introduction

Respiratory failure is a source of considerable mortality and morbidity in ICU patients. Recognizing patients that are at risk of acute respiratory failure early could help clinicians to expedite the commencement of appropriate treatment. Lung function is clinically evaluated using the ratio of blood oxygen partial pressure (PaO_2) and fraction of inspired oxygen (FiO_2), commonly referred to as P/F ratio [2]. A healthy person breathing room air is expected to have a P/F ratio of 475 mmHg (PaO_2 : ~ 100 mmHg, room air FiO_2 : 21 %). Current medical literature defines respiratory failure in three stages [1]:

- **Mild:** $200 \text{ mmHg} \leq \text{P/F} < 300 \text{ mmHg}$
- **Moderate:** $100 \text{ mmHg} \leq \text{P/F} < 200 \text{ mmHg}$
- **Severe:** $\text{P/F} < 100 \text{ mmHg}$

*These authors contributed equally

†Correspondence to TobiasM@adhb.govt.nz and raetsch@inf.ethz.ch

As of yet few approaches using machine learning models to predict respiratory failure in the ICU have been reported. Ding et al. used a random forest classifier to predict patients’ risk of developing acute respiratory distress syndrome from information derived from 42 variables collected during the first day of ICU admission [4], and hence do not provide real-time predictions. Kim et al. proposed FAST-PACE which is based on an LSTM to predict cardiac arrest and respiratory failure 1-6 h prior to adverse clinical events [10], and use a small set of only 9 features, potentially limiting model performance. In this work, we propose an **Early Warning System (EWS)** that can be used to continuously monitor the patients’ respiratory state and alert the clinicians when respiratory failure is impending, using a comprehensive feature set from 25 relevant clinical variables.

2 The HiRID-II dataset

A **High time Resolution ICU Dataset (HiRID)** was curated to train an EWS for circulatory system failure in [6]. The temporal resolution of vital sign data in HiRID is higher than that in MIMIC-III [8] and eICU [12]. The high-resolution data facilitates more frequent predictions of the patient state, which can help ICU clinicians to make critical decisions more rapidly. In this work, we used HiRID-II, an extension of HiRID by including more patient data from 2016 to 2019, to train a machine learning model to perform early prediction of respiratory system deterioration. After the filtering steps shown in Supplementary Figure A.1 were performed, 62551 ICU patient admissions remained. The statistics of development data from HiRID-II are shown in Supplementary Figure B.1. We summarized 322 meta-variables using 899 recorded variables in the database, 189 more than those used in [6]. Each meta-variable was derived from recorded variables with similar medical concepts.

3 Continuous estimation of P/F ratio

The definition of respiratory failure depends on the availability of a current PaO_2 and FiO_2 value. To measure PaO_2 , an arterial blood sample (ABGA) of the patient has to be drawn and processed. Therefore, PaO_2 measurements are only available at intervals determined by the measurement frequency. For a continuous assessment of patient respiratory state using P/F ratio, estimates of PaO_2 values have to be used when its measurements are not available. In the clinical setting, continuously monitored pulse oximetry derived haemoglobin oxygen saturation (SpO_2) can be used to estimate the current PaO_2 value [3, 5, 13]. A comparison of different existing models shows that the non-linear parametric model by Ellis [5, 13] performs best. We were able to further improve continuous PaO_2 estimation using neural networks (NNs). Two PaO_2 estimation models were developed: 1) a basic NN relying only on SpO_2 measurements as input (SpO_2 -NN); 2) a more complex NN that also takes the last ABGA measurement into account (Full-NN).

Table 1: Area under the receiver operating characteristic (AUROC) and median absolute PaO_2 estimation error of the two NNs and the parametric non-linear baseline (pnl-baseline) [5]. The AUROC shows the performance of the models in detecting P/F ratios ≤ 200 mmHg. The best results per category are presented in **bold**, the second best in *italic*.

Range SpO_2 (%)	n	pnl-baseline	SpO_2 -NN	Full-NN
Overall	20994	10.1	<i>9.6</i>	9.2
90-96	7945	6.9	<i>6.8</i>	6.3
80-90	780	6.1	<i>5.1</i>	4.4
70-80	78	19.7	<i>10.2</i>	8.2
AUROC	12823	0.914	<i>0.917</i>	0.919

Table 1 shows that both NNs outperform the best baseline model in absolute estimation error and discriminating patients with and without moderate/severe respiratory failure. We provide more details about the proposed NNs in Appendix C.1.

For the calculation of the P/F ratio, estimates of FiO_2 values are also necessary. Three situations need to be distinguished: 1) the patient is breathing ambient air, i.e. $\text{FiO}_2 = 21\%$ (the ambient air oxygen fraction); 2) for patients receiving supplemental oxygen FiO_2 is estimated using the lookup table by [14] (see Supplementary Table C.4); 3) for patients on mechanical ventilation FiO_2 is controlled by the ventilator and its value is recorded in the data.

Here we are interested in predicting respiratory failure of only the moderate/severe level as previously defined. Therefore, a time point t is labeled as positive for respiratory failure if the following conditions are true for two thirds of a two-hour forward window (see Figure 1b):

- P/F ratio < 200 mmHg;

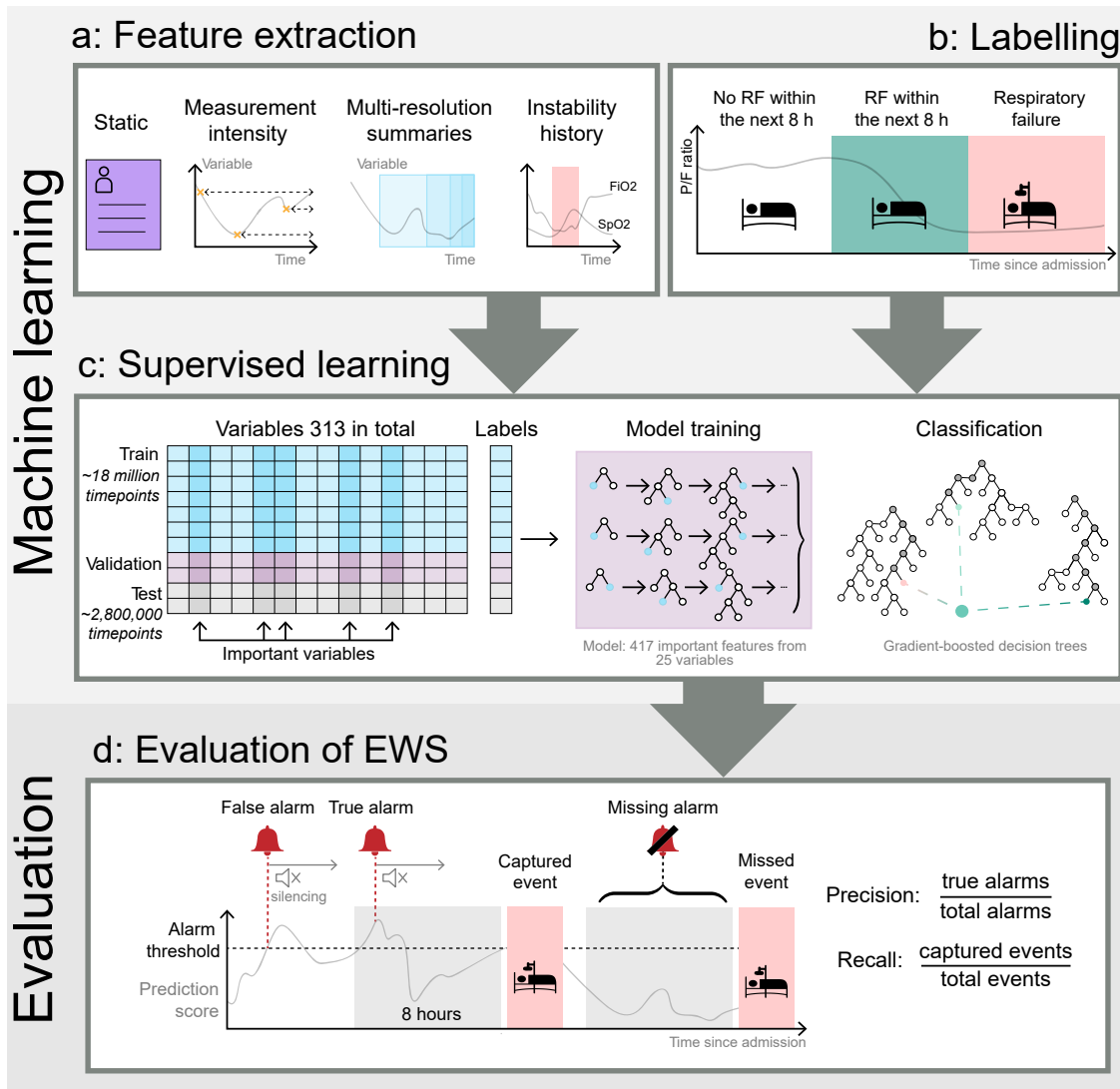


Figure 1: Workflow diagram of the respiratory EWS.

- for mechanically ventilated patients: the positive end expiratory pressure (PEEP) is ≥ 5 mmHg.

To remove spurious detections, we merged successive events with a gap of at most 1h into one event, and deleted short events of length at most 2h. Our model then predicts the patient being in respiratory failure in the next 8h according to the above definition, given they are currently stable, which implements an early warning system.

4 Early warning system for low P/F ratio

As an initial step, the 20 most influential variables for predictions were retrieved on a basic feature set including measurement intensity and the current parameter value using SHAP value analysis [11], and augmented with clinically important variables, yielding $n_{\text{var}} = 25$ variables used for model development.

To give our model a comprehensive view of the patient state the following feature classes were extracted (see Figure 1a) on these variables:

- **Current value:** The current parameter value.
- **Multi-resolution summary:** The summary functions {mean, std, trend, min, max} were computed over the last 8 hours as well as the entire stay up to now.

- **Measurement intensity:** The time to last real measurement, measurement density in the last 8 hours as well as during the entire stay up to now.
- **Instability history:** If applicable for a variable, up to 3 severity levels were annotated using prior medical knowledge. The fraction of time spent in each severity state over the last 8 hours as well as over the entire stay up to now was extracted.

Static variables were used directly as a feature.

These features were then passed to an ensemble of decision trees implemented in LightGBM [9], shown in Figure 1c. Trees were added to the ensemble until performance did not improve for 50 epochs in the validation set, early stopping the training process. Prediction scores were generated for patients in the test set, and form the basis of the early warning system.

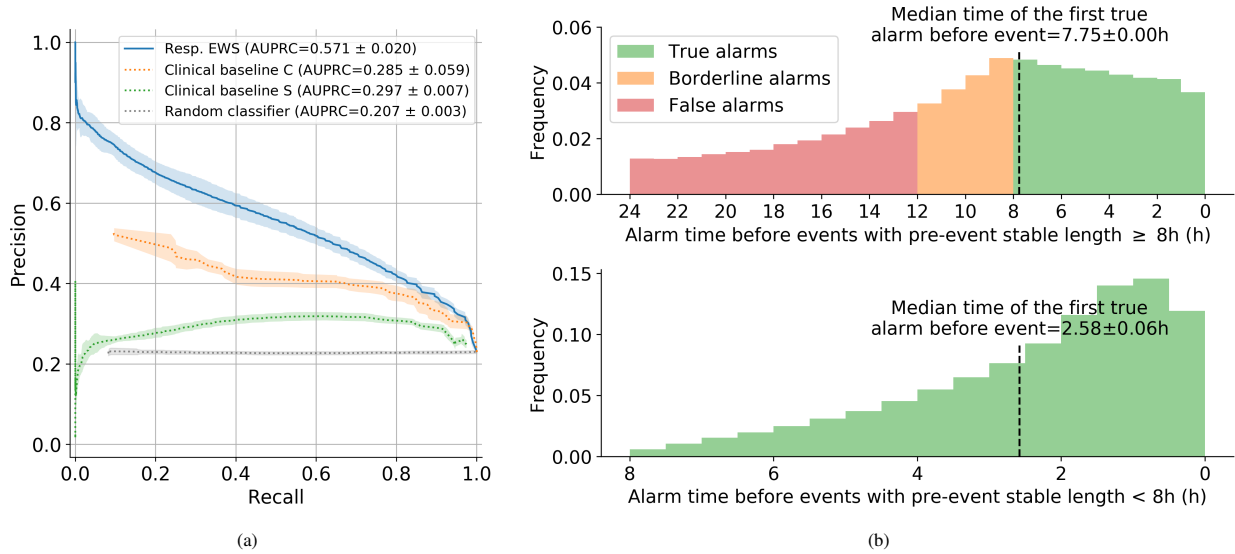


Figure 2: (a) Event-based precision-recall curve of EWS for acute respiratory failure, two clinical baselines and a random classifier. **Clinical baseline S** is a simple baseline solely based on SpO₂ lower than the specified threshold. **Clinical baseline C** is a more complex baseline that uses a single decision tree trained on two basic features, the current estimate of SpO₂ and FiO₂, with at most 32 leaves. **Random classifier** shows the event prevalence. Both baselines and the random classifier also use the same alarm silencing strategy as our method. Error bands show the standard deviation of model performance in 5 separate data splits, similar to [6]. (b) Distribution of alarm time before respiratory failure. The median time of the first true alarm before all events irrespective of the pre-event stability length is 3.75 ± 0.24 h.

The conventional way of evaluating the performance of machine learning models for time-series is using a time-point based precision-recall curve. This is less suitable for clinical settings because it is equivalent to evaluating a system that generates frequent alarms, which can cause alarm fatigue that should be avoided in healthcare settings [7]. We used the alarm silencing strategy proposed by Hyland et al.[6], which silences further potential alarms within a specified period of time after the model output triggers an alarm, hence reducing alarm fatigue. In our evaluation, we use 30 minutes as the alarm silencing time. The same event-based precision and recall definition proposed in [6] was adopted (see Figure 1d).

Figure 2a shows that our respiratory EWS outperforms the two clinical baselines significantly, and that it only generates 3 false alarms out of 5 alarms at 80% recall, with the first alarm alerting the clinicians to future respiratory failure occurring on average approximately 4 hours before the actual event, given the event was detected (see Figure 2b). The average number of alarms within the 8-hour window prior to detected respiratory failure events is 7.4, meaning that the systems will keep informing the clinicians roughly every hour in this period before respiratory failure.

5 ICU monitor

To aid model introspection and diagnostics we have developed a user customizable, web-based tool for interactive data exploration of the HiRID time-series data, generated features and model predictions. The system supports the manual annotation of arbitrary time series tracks. This gives clinicians the opportunity to visually discover the data and perform

actions such as annotation of interesting regions in the data, or annotation of wrong predictions, putting the clinician into the model improvement loop. For more details about the tool, we refer to the Appendix F.

6 Conclusion

In this work, we describe the development of an early warning system for respiratory failure in the ICU setting. In a first step, we successfully derived a non-parametric model for PaO₂ estimation based on continuously available SpO₂ measurements and previous ABGA data, which outperforms the best baseline method. The PaO₂ model allows for the continuous estimation of the patient respiratory state without frequent ABGA, and also enables the continuous state definition needed for training an early warning system for respiratory failure. Our model predicts respiratory failure in real time and can alert clinicians early with a lower false alarm rate to impending respiratory failure than the clinical baselines. We hypothesize that our system can facilitate early reassessment of a deteriorating patient, enabling the rapid treatment and improving patient outcomes. Our approach allows for feature inspection on individual prediction and SHAP value analysis of important predictors, offering additional valuable insights to clinicians. Our visualization tool enables the visual exploration of the relevant variables and the system's predictions. Future work will investigate alternative definitions of moderate/severe respiratory failure, as well as exploring alternative modeling choices, including different machine learning models.

Acknowledgments

This project was supported by the Grant No. 205321_176005 of the Swiss National Science Foundation (to TMM/GR) and ETH core funding (to GR).

References

- [1] ARDS Definition Task Force, V Marco Ranieri, Gordon D Rubenfeld, B Taylor Thompson, Niall D Ferguson, Ellen Caldwell, Eddy Fan, Luigi Camporota, and Arthur S Slutsky. Acute respiratory distress syndrome: the berlin definition. *JAMA*, 307(23):2526–2533, June 2012.
- [2] Gordon R Bernard, Antonio Artigas, Kenneth L Brigham, Jean Carlet, Konrad Falke, Leonard Hudson, Maurice Lamy, Jean Roger Legall, Alan Morris, and Roger Spragg. The american-european consensus conference on ards. definitions, mechanisms, relevant outcomes, and clinical trial coordination. *American journal of respiratory and critical care medicine*, 149(3):818–824, 1994.
- [3] Samuel M Brown, Abhijit Duggal, Peter C Hou, Mark Tidswell, Akram Khan, Matthew Exline, Pauline K Park, David A Schoenfeld, Ming Liu, Colin K Grissom, Marc Moss, Todd W Rice, Catherine L Hough, Emanuel Rivers, B Taylor Thompson, Roy G Brower, and National Institutes of Health (NIH)/National Heart, Lung, and Blood Institute (NHLBI) Prevention and Early Treatment of Acute Lung Injury (PETAL) Network. Nonlinear imputation of PaO₂/FIO₂ from SpO₂/FIO₂ among mechanically ventilated patients in the ICU: A prospective, observational study. *Crit. Care Med.*, May 2017.
- [4] Xian-Fei Ding, Jin-Bo Li, Huo-Yan Liang, Zong-Yu Wang, Ting-Ting Jiao, Zhuang Liu, Liang Yi, Wei-Shuai Bian, Shu-Peng Wang, Xi Zhu, et al. Predictive model for acute respiratory distress syndrome events in icu patients in china using machine learning algorithms: a secondary analysis of a cohort study. *Journal of Translational Medicine*, 17(1):326, 2019.
- [5] R K Ellis. Determination of PO₂ from saturation. *J. Appl. Physiol.*, 67(2):902, August 1989.
- [6] Stephanie L Hyland, Martin Faltys, Matthias Hüser, Xinrui Lyu, Thomas Gumbsch, Cristóbal Esteban, Christian Bock, Max Horn, Michael Moor, Bastian Rieck, et al. Early prediction of circulatory failure in the intensive care unit using machine learning. *Nature Medicine*, 26(3):364–373, 2020.
- [7] ERCI Institute. Top 10 technology hazards for 2012: the risks that should be at the top of your prevention list. *Health Devices*, 40(11):358–373, 2011.
- [8] Alistair EW Johnson, Tom J Pollard, Lu Shen, H Lehman Li-Wei, Mengling Feng, Mohammad Ghassemi, Benjamin Moody, Peter Szolovits, Leo Anthony Celi, and Roger G Mark. MIMIC-III, a freely accessible critical care database. *Scientific data*, 3(1):1–9, 2016.
- [9] Guolin Ke, Qi Meng, Thomas Finley, Taifeng Wang, Wei Chen, Weidong Ma, Qiwei Ye, and Tie-Yan Liu. LightGBM: A highly efficient gradient boosting decision tree. In *Advances in neural information processing systems*, pages 3146–3154, 2017.

- [10] Jeongmin Kim, Myunghun Chae, Hyuk-Jae Chang, Young-Ah Kim, and Eunjeong Park. Predicting cardiac arrest and respiratory failure using feasible artificial intelligence with simple trajectories of patient data. *Journal of clinical medicine*, 8(9):1336, 2019.
- [11] Scott M Lundberg and Su-In Lee. Consistent feature attribution for tree ensembles. *arXiv preprint arXiv:1706.06060*, 2017.
- [12] Tom J Pollard, Alistair EW Johnson, Jesse D Raffa, Leo A Celi, Roger G Mark, and Omar Badawi. The eicu collaborative research database, a freely available multi-center database for critical care research. *Scientific data*, 5:180178, 2018.
- [13] J W Severinghaus. Simple, accurate equations for human blood O₂ dissociation computations. *J. Appl. Physiol.*, 46(3):599–602, March 1979.
- [14] Richard B Wettstein, David C Shelledy, and Jay I Peters. Delivered oxygen concentrations using low-flow and high-flow nasal cannulas. *Respir. Care*, 50(5):604–609, May 2005.

A Patient and variable flow chart

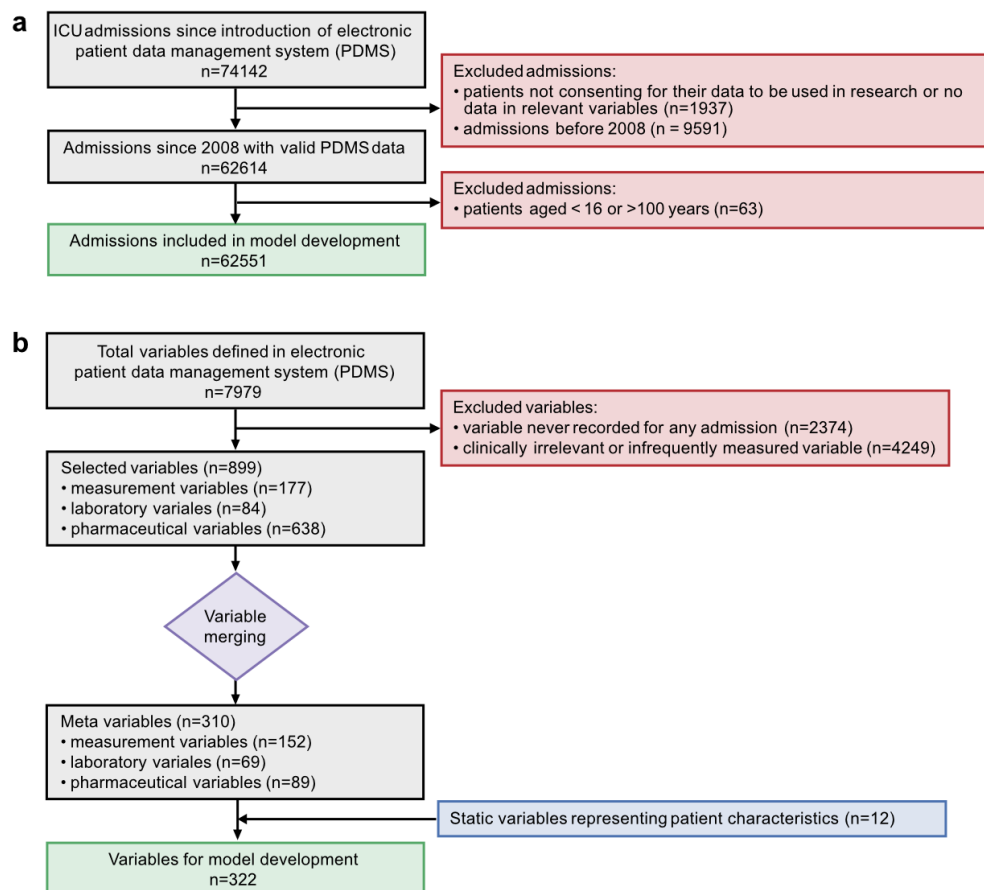


Figure A.1: a, Flow chart of the exclusion criteria applied to the HiRID-II patient cohort. b, Flow chart of the exclusion, merging, and post-processing applied to the variables in the patient data management system

B HiRID-II patient cohort statistics

Sex			
Male	62.45 %	35002 admissions	
Female	37.55 %	21045 admissions	
Age (years)			
Median (Mean)	65 (62.14)		
Range	16-100		
Length of stay (days)			
Median (Mean)	0.94 (2.20)		
Range	0-98		
Admission type			
Emergency	59.38 %	33280 admissions	
Not emergency	38.67 %	21672 admissions	
Unknown	1.95 %	1096 admissions	
Surgical status			
Yes	50.12 %	28092 admissions	
No	47.02 %	26355 admissions	
Unknown	2.86%	1601 admissions	
APACHE diagnostic group			
<i>Cardiovascular</i>			
	Surgical	19.88 %	11144 admissions
	Nonsurgical	10.82 %	6062 admissions
<i>Neurological</i>			
	Surgical	13.84 %	7759 admissions
	Nonsurgical	20.01 %	11216 admissions
<i>Respiratory</i>			
	Surgical	1.67 %	934 admissions
	Nonsurgical	7.17 %	4019 admissions
<i>Trauma</i>			
	Surgical	0.93 %	522 admissions
	Nonsurgical	5.43 %	3041 admissions
<i>Other</i>			
		20.25 %	11351 admissions
Respiratory dysfunction			
Patients with events	59.96 %	33872 admissions	
Mean #events per patient with events	2.49		
Mean event duration	631 minutes		
Mean time to first event	866 minutes		
Mortality			
	5.37 %	3012 admissions	

Figure B.1: Statistics of the development cohort extracted from the HiRID-II database

C Continuous P/F ratio estimation

C.1 PaO₂ estimation model development

Both the SpO₂-NN and Full-NN models are trained using the HiRID dataset [6], which contains 196,148 arterial blood gas analysis (ABGA) samples. We split the ICU admissions with using 75%/25% training/test ratio. The training set contains 147'210 ABGA samples from 19'419 ICU admissions, and the test set contains 48'938 ABGA samples from 6'473 ICU admissions. Before training we excluded a total of 32'210 ABGA samples (30'537 due to value being outside of the normal PaO₂ range [40, 250] mmHg and 1'673 due to the last ABGA measurement being longer than 24h in the past).

We applied cross-validation and used grid search in hyperparameter tuning for both proposed NNs. We summarize the hyperparameters as well as their search space in Table C.1, and also show the best hyperparameter set selected for each proposed NN in C.2. The best set of hyperparameters was chosen based on the lowest mean absolute prediction error in the clinically relevant region of SaO₂ < 96%.

For the more complex model, Full-NN, we first train it on a large variable set consisting of SaO₂, mean etCO₂ (10 min), mean patient body temperature (4 hours) and different measurements from the previous ABGA test (namely SaO₂, pH, FiO₂, PaO₂, Hb, MetHb, COHb, pCO₂, BE, HCO₃ and lactate). We then performed a greedy backward selection with 3-fold cross validation to select the most important variables from the initial variable set. The four most important variables are the current and the last SaO₂, as well as PaO₂ and pH from the last ABGA test. It is important to note that the models were trained using SaO₂ as input for the haemoglobin oxygen saturation, which is the corresponding precise measure of haemoglobin oxygen saturation in an ABGA. As this value hence is also not continuously available, we had to use the less precise, but continuously available SpO₂ during prediction. The evaluation on the test set was done using SpO₂ to reflect the use case. All model development was performed with Tensorflow 1.15.

Table C.1: Hyperparameters for the proposed NNs and their search space. **Hidden layer nodes:** each element n in the tuple represents a hidden layer with n nodes. **Weight correction factor γ :** let x_i be the SaO₂ value of the i -th training example, and we define $c := |\{x_j = x_i | j \in \{1, \dots, N_{\text{train}}\}\}|$. During training the cost of the i -th training example is multiplied by $1/c^\gamma$. **Dropout rate:** the fraction of nodes being randomly dropped out in each hidden layer during training.

Hyperparameter	Search space
Batch size	{30, 50, 100, 300, 500}
Hidden layer nodes	{(8,8), (16,16), (32,32), (64,64), (128,128), (256,256), (64,128), (128,64), (64,64,64), (64,128,64), (128,128,128), (128,256,128), (256,512,256)}
Weight correction factor γ	{None, 0.1, 0.2, 0.33, 0.5, 1}
Learning rate	$[10^{-4}, 10^{-1}]$ (10 grid points)
Dropout rate	$[0, 0.5]$ (10 grid points)

Table C.2: The best hyperparameters selected for the two PaO₂ estimation NNs

Model	Selected hyperparameters
SpO ₂ -NN	Batch size: 50; Hidden layer nodes: (64,128,64); Weight correction factor: None; Learning rate: 0.0001; Dropout rate: 0.5
Full-NN	Batch size: 50; Hidden layer nodes: (8,8); Weight correction factor: 0.2; Learning rate: 0.001; Dropout rate: None

C.2 PaO₂ estimation model performance

Table C.3: Area under the receiver operating characteristic (AUROC) and median absolute PaO₂ estimation error of the two NNs and the parametric non-linear baseline (pnl-baseline) [5]. The AUROC shows the performance of the models in detecting P/F ratios \leq 200 mmHg. The best results per category are presented in **bold**, the second best in *italic*.

Range SpO ₂ %	n	pnl-baseline (iqr)	SpO ₂ NN (iqr)	Full NN (iqr)
0-100	20994	10.1 (16.1)	<i>9.6 (15.0)</i>	9.2 (14.8)
0-96	8813	6.8 (9.9)	<i>6.7 (10.3)</i>	6.1 (9.8)
96-100	12181	13.8 (19.1)	<i>12.4 (17.5)</i>	12.3 (17.2)
90-96	7945	6.9 (9.9)	<i>6.8 (10.2)</i>	6.3 (9.9)
85-90	636	5.8 (8.3)	<i>5.3 (6.9)</i>	4.4 (6.7)
80-85	144	7.2 (15.8)	<i>4.8 (11.5)</i>	4.7 (10.4)
75-80	63	14.6 (38.2)	<i>7.1 (35.9)</i>	6.7 (32.9)
60-75	22	29.5 (52.5)	<i>17.5 (55.0)</i>	14.0 (52.1)
auROC	12823	0.914	<i>0.917</i>	0.919

C.3 FiO₂ estimation

Table C.4: Supplemental Oxygen to FiO₂ conversion table used for determining the continuous FiO₂ estimate.

Supp. oxygen [l]	FiO ₂ [%]	Supp. oxygen [l]	FiO ₂ [%]
1	26	9	63
2	34	10	66
3	39	11	67
4	45	12	69
5	49	13	70
6	54	14	73
7	57	15	75
8	58	>15	75

D Variable selection and model introspection

Table D.1: List of the 20 most important variables according to SHAP value analysis, as well as additional variables, which are plausible given prior medical knowledge. The ranking was determined by ranking the features using the mean absolute SHAP value in the validation set, and then ranking the variables by the rank of their most important feature. The 25 displayed variables formed the basis of the proposed prediction model.

Rank	Important variable	Rank	Important variable
1	FiO ₂	11	Spontaneous breathing?
2	SpO ₂	12	Admission origin
3	Supplemental oxygen	13	GCS Motor
4	PaO ₂	14	Weight
5	Supplemental FiO ₂ %	15	Ventilator mode group
6	SaO ₂	16	RASS
7	GCS Eye opening	17	Patient age
8	GCS Response	18	Extubation time-point
9	Peritoneal dialysis	19	Tracheotomy state
10	Peak pressure	20	ST2 (ECG)

Clinically identified variables	
	Respiratory rate
	PEEP
	OUT
	Current FiO ₂ estimate
	Ventilation state

Table D.2: Most important features identified by SHAP analysis in the validation set of the 6 splits. The ranking was obtained by first finding the mean of absolute SHAP values for all samples in the validation set of a split, and then averaging this mean across all splits.

Rank	Important feature
1	SpO ₂ (Mean 8h)
2	FiO ₂ estimate (Current value)
3	FiO ₂ estimate (Max 8h)
4	FiO ₂ estimate (Mean 8h)
5	FiO ₂ estimate (Mean entire stay)
6	SpO ₂ (Current value)
7	SpO ₂ (Mean entire stay)
8	Ventilator peak pressure (Current value)
9	SpO ₂ (Instable density of L1 90-94 % 8h)
10	FiO ₂ (Instable density of L1 30-40 % 8h)
11	Peritoneal dialysis (Time to last ms.)
12	FiO ₂ estimate (Std. entire stay)
13	PaO ₂ (Current value)
14	Supplemental oxygen (Instable density of L1 2-4 l/min 8h)
15	GCS Eye opening (Current value)
16	PaO ₂ (Min 8h)
17	Supplemental FiO ₂ % (Instable density of L1 21-40 8h)
18	Peritoneal dialysis (Meas. density entire stay)
19	FiO ₂ (Current value)
20	Patient age

E ROC-based performance of the prediction score

For completeness, we also display an evaluation of the proposed Resp EWS prediction score using the classical way of time-point based evaluation using ROC analysis. Sensitivity is the fraction of correctly retrieved time points at which an alarm is mandated, in the 8 hours before respiratory failure. Specificity is the fraction of time-points at which no alarm should be produced, in which indeed none is produced. Optimal performance under this evaluation implies producing an alarm every 5 minutes.

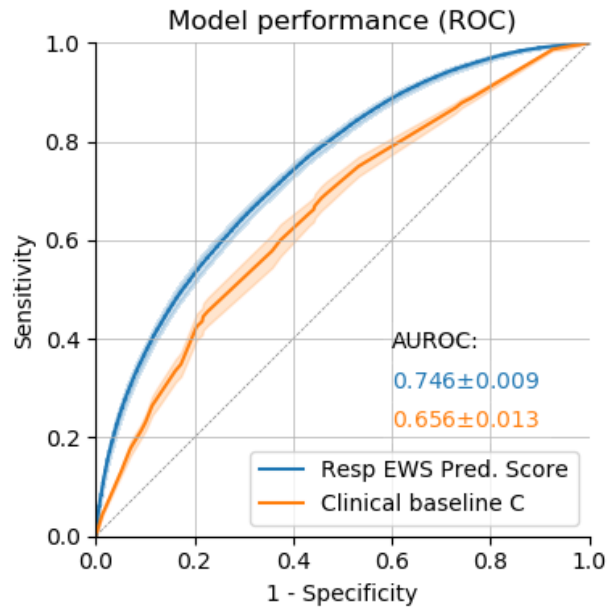


Figure E.1: ROC curve of the Resp EWS prediction score underlying the proposed alarm system.

F ICU monitor: patient data visualization

We have developed a flexible and dynamic web-based viewer for the HiRID-II time-series data, as well as auxiliary data generated during experiments. Arbitrary channels can be plotted in vertically arranged line or scatter plots, where the x-axes are the date-times of the measurements, and kept synchronized during interactive/animated zoom and pan operations. We use the tool for the exploration and inspection of data across many patients, and for the overlay and evaluation of derived events and quantities relevant to experimentation, like event annotations or machine learning labels. We plan to share the tool under an open source license, and we describe some of its current features below.

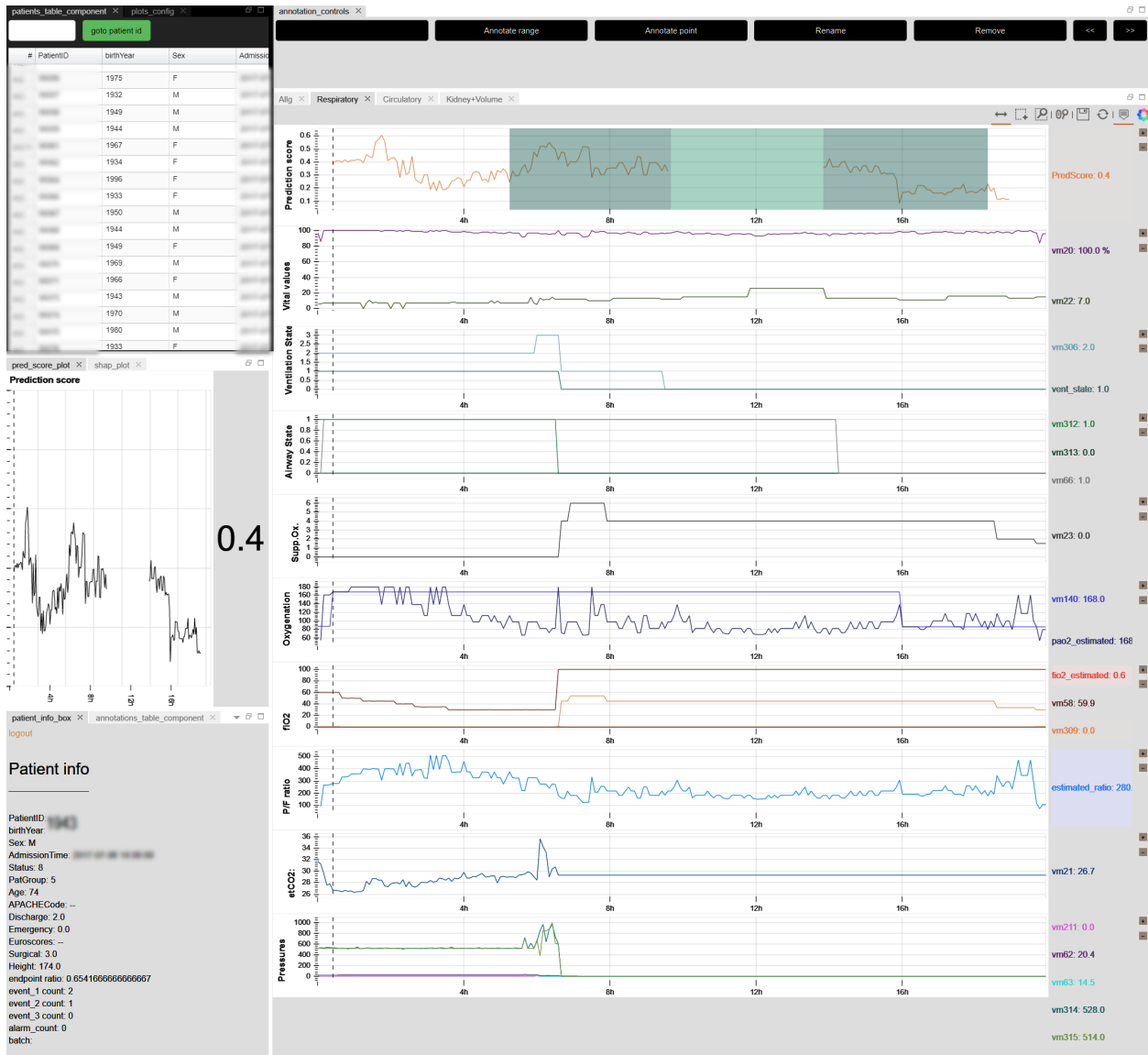


Figure F.1: Illustrative print screen of the newly developed ICU monitor tool for data inspection. The topmost graph is displaying the models' predicted score. The underlaid regions mark event levels of different severity. The light green region represents a respiratory failure state, therefore no predictions are produced during this period. The other graphs show a customizable selection of the variables. Regions of the ICU monitor displaying patient ID and exact dates are blurred-out.

F.1 Visualization features

- Arbitrary time-resolution (x-axes ticks intelligently adjust to different time scales)
- Irregular time-steps (for example, we overlay post-processed data at a regular time interval on top of source data with irregular time steps)

- Missing data (missing points are not rendered)
- Auto-scaling y-ranges, overridable by configuration
- Inspect exact values by hover tooltip, or by moving a “current timestep” cursor
- Auto color allocation per channel, and readouts with channel label and unit, according to current cursor position
- Dynamically sizable heights of individual plots
- Multiple channels per plot, up to 2 y-axes per plot
- Distribution of plots to separate named tabs
- Dynamic resize and popout of tabs (e.g. for viewing on a second monitor)
- Distribution of channels to plots, and plots to tabs are both reconfigurable “live” without restarting/reloading
- Full sortable table of patients, click or type in patient ID to load a patient
- Patient info listing, with list of available channels available for use in plot configuration

F.2 Event annotation features

- Overlay of “annotations” / “events” for time ranges or time points
- Live modification of annotation/event color per annotation/event type, via the UI
- Events loaded statically from data files, or annotations added interactively via UI
- Keyboard shortcuts for streamlined use of mouse for both annotation time range selection as well as zoom & pan
- Display of annotation/event labels/names on the plots
- JSON-schema defined schema per annotation/event type, allowing entry of structured metadata per annotation/event in the UI
- Display and edit metadata in a dynamic form in the UI, and view metadata in special hover tooltip mode
- Dump metadata of annotations/events to JSON via predefined route/URL
- Sortable and filterable table of annotations/events, selecting a row automatically pans the x-axis such that the annotation/event comes into view
- Chronological navigation of annotations/events using the arrow keys
- Filtering annotations/events to only certain types of interest (filtered types will be hidden from view and be skipped when navigating chronologically)
- Selection of annotations/events by mouse-click, synchronized to the table, and supporting unambiguous behavior for selection on overlapping annotations/events
- Keyboard shortcuts for remove/rename annotation